

Alternate Thermomechanical Heat Treatment Cycles for the Enhancement in Hardness and Tensile Properties of Commercial Grade AA6061

Ramakrishna Vikas Sadanand^a, Sathyashankara Sharma^{a*} , P. R. Prabhu^b

^aManipal Academy of Higher Education, Manipal Institute of Technology, Department of Mechanical and Industrial Engineering, Manipal, Karnataka, 576104, India.

^bManipal Academy of Higher Education, Manipal Institute of Technology, Department of Mechatronics, Manipal, Karnataka, 576104, India.

Received: February 1, 2022; Revised: September 27, 2022; Accepted: October 17, 2022

Numerous research incorporating precipitation hardening and/or strain hardening on Al-Mg-Si alloys has demonstrated improved mechanical properties in the alloys. However, there is a lack of research on how these processes can be combined efficiently to provide better strength and hardness for the alloys. The present study describes the effects of low temperature thermomechanical treatment (LTMT - combination of conventional age hardening and strain/work hardening) carried at two isothermal aging temperatures on the hardness and strength of the aluminium alloy 6061 (AA6061). Further, an innovative LTMT process is also proposed, which aims at further enhancing the mechanical properties of the alloy. The study revealed the increase in degree of deformation improved the strength and hardness of the alloy with reduced aging time. The effect of the degree of deformation, pre-deformation, and alternate deformation and aging cycles on the hardness and strength of the alloy was studied with the help of fracture surface analysis.

Keywords: AA6061, Al-Mg-Si alloy, Low Temperature Thermomechanical Treatment, Hardness, Cold Rolling, Fractography.

1. Introduction

In the present scenario, materials with high strength, hardness, and ductility, along with prolonged service life at low cost, are the prime requirements in all advanced engineering sectors. The beneficial properties provided by precipitation hardenable aluminium alloys include low density, superior mechanical strength, improved stiffness, high toughness, corrosion resistance, excellent formability, and weldability among others¹⁻⁴. These invaluable properties broaden the applicability of the alloy for heavy structural functions in the fields of marine, mining, aerospace, military, and automobile. The necessity for lightweight, high strength-to-weight ratio, high modulus-to-density ratio, and excellent performance, which are further tailorable, was the primary guiding force for the development of new methodologies and techniques to process AA6061.

In recent times, 6xxx (Al-Mg-Si based) alloys and, more specifically, AA6061 has been extensively studied by intentional deformation techniques to achieve grain refinement⁵⁻⁸. Processing of bulk materials through various severe plastic deformation techniques such as equal channel angular pressing⁹⁻¹¹, accumulative roll bonding¹²⁻¹⁴ and high-pressure torsion^{15,16} have also been applied. The reason for the study has been to obtain the combination of ductility and strength which can only be achieved in case of precipitation hardenable alloys by deformation followed by aging treatment. The response of 6xxx series alloys to age hardening is significant and leads

to exceptional enhancement of the strength following an appropriate heat treatment process. The precipitation sequence which aids the strengthening of the alloy has been reported in numerous studies, and acceptable results after phase evolution occurring during aging have been achieved¹⁷⁻²¹. The complex precipitation sequence of AA6061 during aging involves many intermediate stages²². The sequence and the type of phases for a particular aging temperature are dependent on the composition which in turn are determined by equilibrium phases. Furthermore, the development of crystallographic structures through plastic deformation combined with aging can offer tailored properties in the alloy²³.

The current work aims to study the influence of conventional aging, and thermomechanical treatments on the hardness and tensile properties of the AA6061. In addition, a modified version of thermomechanical treatment was also implemented on the alloy to research its effects on the hardness and tensile properties of the alloy. The fracture analysis of the tensile specimens is carried out to understand the failure mode of the alloy.

2. Methodology

The material selected for the study is commercially available AA6061 which is a widely used 6XXX series aluminium alloy. The alloy in as-bought condition was tested for its composition through spectroscopic analysis, which showed higher amounts of magnesium and silicon. The analysis revealed the presence of 0.25% Fe, 0.19% Cu,

*e-mail: ss.sharma@manipal.edu

0.07% Mn, 0.73% Si, 0.95% Mg and 0.06% Ti by weight in the alloy. The AA6061 alloy billets were melted in the electric resistance heat furnace at 750°C. After the billets had completely melted, the impurities were removed in the form of slag. The melt was poured into the preheated (at 500°C) cast-iron permanent moulds, allowed to cool, and solidify.

2.1. Heat treatment of AA6061

The AA6061 alloy castings were machined and cut to produce specimens with appropriate dimensions for hardness and tensile tests. The specimens were subjected to precipitation hardening (Figure 1a) and low temperature thermomechanical treatment (Figure 1b). The precipitation hardening (conventional heat treatment) involved:

1. Soaking of the specimens at 550°C for a duration of 2 h,
2. Immediate quenching in water at room temperature, and
3. Artificial aging of the quenched specimens in a hot air oven at isothermal aging temperatures (IATs) of 100 and 180°C to attain peak hardness.

The low temperature thermomechanical treatment (LTMT) was carried out on specimens with three different deformation densities. The LTMT carried out on the specimens involved:

1. Soaking of the specimens at 550°C for a duration of 2 h,
2. Immediate quenching in water at room temperature,
3. Cold rolling of the quenched specimens to produce required degree of deformation through the reduction in thickness, and
4. Artificially aging the rolled specimens in hot air oven at IATs of 100 and 180°C to attain peak hardness.

The rolling was carried out to reduce the thickness of the specimens by 4, 8 and 12%, wherein each specimen is rolled with several passes to achieve the final reduction in thickness. The LTMT process was carried out to find the peak hardness of the cast alloy with different deformation densities. Table 1 provides the details of the individual specimen thickness before and after the cold rolling process. In each case, 20-25 specimens were prepared to measure the peak hardness and 5 specimens were prepared at peak aged conditions to measure the tensile strength of the alloy.

The cast AA6061 specimens were also subjected to a completely new and different thermomechanical treatment process. This new LTMT (nLTMT) process (Figure 2) involved alternate rolling and aging process carried out in two steps. The amount of the deformation (C_1 & C_2) as shown in Figure 2 in both the stages, are half the total deformation. For example, if the total deformation carried out in the LTMT process was 4%, then the deformation for the nLTMT process was 2% in each of the two steps. Similarly, the aging time (D_1 & D_2) as shown in Figure 2 in both the stages, are at different ratios of 1:1, 1:2 and 2:1, respectively. The total of the two aging times selected in each step was equal to the corresponding aging time which achieved the peak hardness for the LTMT specimens.

2.2. Hardness and tensile test

Vickers hardness testing machine with a diamond indenter (pyramid-shaped - 136° angle) was used to conduct the hardness test. The hardness was measured under a load of 100 kgf applied for 15 s following the ASTM E384 standard. The hardness test was carried out wherein an average of a minimum of five indentation readings from different locations were considered for each specimen. This procedure was employed to ensure the consistency of the results. The scattering of hardness values is observed to be between ± 5 HV.

A horizontal bench model universal testing machine with 20 kN capacity was used to conduct the tensile test. Based on the ASTM B557M – 15 standard the tensile specimens were prepared as shown in Figure 3. The load cell value was maintained at 20.5 kN, and test mode was set to break. The cross-head speed was maintained at a value of 10 mm/min, and specimen was fixed firmly using the gripper.

Table 1. Details of the rolled specimens.

Sl. no.	Initial thickness (mm)	Final thickness (mm)	Average deformation (%)
1	3.12	3	4
2	3.26	3	8
3	3.4	3	12

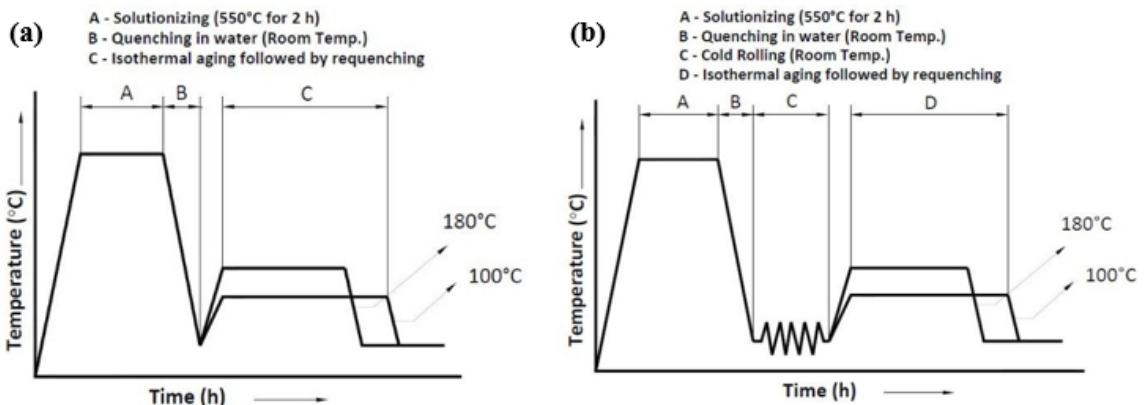


Figure 1. (a) Aging heat treatment cycle for AA6061. (b) Low temperature thermomechanical treatment cycle for AA6061.

The peak-aged condition specimens were used for the tensile test, and an average of three test results are considered for each specimen. The scattering of ultimate tensile strength (UTS) values is observed to be between ± 12 MPa.

3. Results and Discussion

3.1. Mechanical characterization of the cast alloy

The hardness test for AA6061 as-cast, solutionized and heat-treated specimens were carried out using a Vickers hardness tester. The test results revealed 63.9 and 57.43 HV as hardness values for the as-cast and solutionized specimens, respectively. Hardness value of 56 HMV (Micro Vickers Hardness) immediately after solutionizing of 6061 Al-alloy

at 530°C for 4 h was observed by Demir and Gunduz while studying the effects of aging on machinability of the alloy²⁴. Similarly, the Vicker hardness of 6061 aluminium alloy solutionized at 500°C for 2 h was in the range of 50-55 HV as obtained by Ozturk et al.²⁵. It is observed that the quenching of the specimens from solutionizing temperature resulted in significantly softer specimens in comparison to the as-cast specimen. This is the result of the solid solution retained in the form of supersaturated (SS) solid solution as the specimens are quenched from the solutionizing temperature²⁶.

Figures 4a and 4b show the hardness distribution graphs as a function of aging time for AA6061 alloy with deformation (rolling) of 0, 4, 8 and 12%, aged at IATs of 100 and 180°C, respectively. The hardness distribution graphs show gradual increase in hardness with aging time, were the hardness increases, reaches a maximum (peak) value and later decreases. This is a normal behaviour in case of aluminium alloy during aging²⁵.

The properties of the precipitation hardened specimens show improvement as they rely on diffusion kinetics. The diffusion kinetics is the function of mainly the temperature but also depends on strain incurred in the lattice, which depends on the density of nucleation sites which is essential for the formation of new secondary phases²⁷. Throughout the isothermal aging the solute atoms separate out from the SS alloy phase to form solute rich precipitates, which increases the hardness of the alloy.

In the case of the cold rolled specimen, the degree of deformation is a clear indicator of the formation of the nucleation sites. The increase in the degree of deformation brings about an increase in the number of nucleation sites available to create new phases. This aids in the formation of large number of precipitates that affects the growth process resulting in creation of finer grains. Concurrently, the deformation increases the lattice strain caused by the formation of a large number of dislocations, grain boundaries, vacancies, and stacking faults²⁸. This led to the formation of numerous nuclei closer to each other, reducing the aging time to achieve peak hardness. Many studies that involve solution treatment, rolling and/or aging have shown similar trends with respect to increase in hardness and strength of the alloy^{2,22,29-33}.

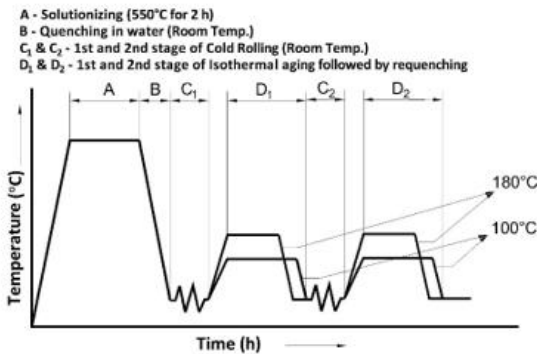


Figure 2. New Low temperature thermomechanical treatment (nLTMT) cycle for AA6061.

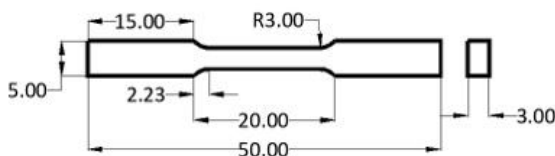


Figure 3. Tensile specimen as per ASTM B57M - 15.

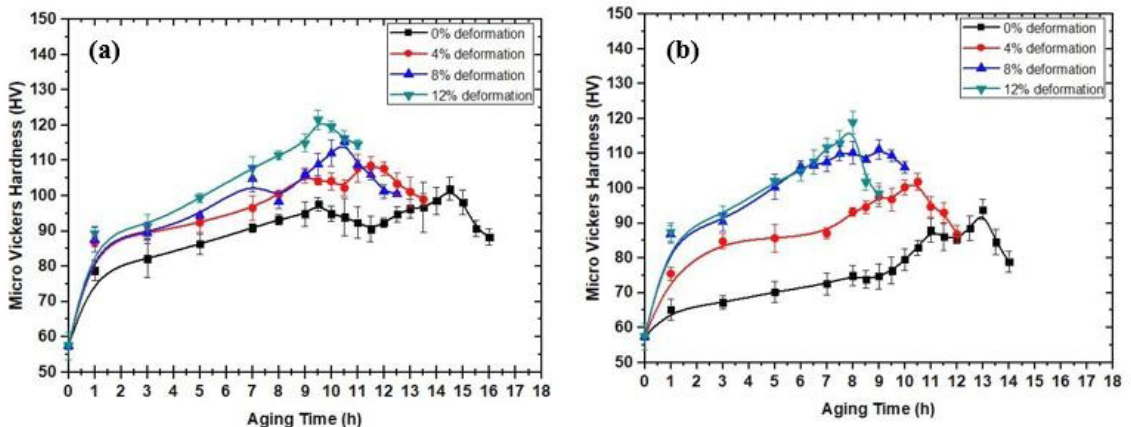


Figure 4. Variation in hardness with aging time for AA6061 specimens aged at (a) 100°C and (b) 180°C.

There is a tendency for two peaks to occur during aging at both the IATs, which was apparent and more noticeable at lower deformation densities of 0 and 4%. Moreover, the distinguished peaks are observed notably at lower aging temperature than higher aging temperature. In aluminium alloys, such phenomena are common, where spontaneous aging occurs with several intermediate stages²². Intermediate stages during aging are plentiful at lower temperatures and lower deformation densities. In these stages, the GP (Guinier–Preston) zones formed from the SS solid solution slowly reform into thermodynamically stable matured secondary phases (intermetallics) with a maximum strain in the lattice at peak aging duration. Higher the degree of deformation, higher is the crystal defects for heterogeneous phase transformation from SS phase; hence, shorter is the time for peak aging. Similarly, higher the aging temperature, faster is the diffusion rate, and lesser is the time for peak aging. Also, lower aging temperature results in more heterogeneous intermediate metastable phases formed with continuous increase in the lattice strain at each step of the phase modification reflected as high peak hardness values.

Table 2 shows the peak hardness values and the corresponding aging time of alloys subjected to precipitation hardening and LTMT at two IATs. The peak hardness values of the alloy at both the IATs show a considerable increase in hardness. At 100°C, the peak hardness of the alloy increased to a maximum value of 120.07 HV, which is 17% higher than the hardness of the undeformed alloy. While at 180°C, the peak hardness achieved for the alloy was 118.83 HV, which is 26% higher than the hardness of the undeformed alloy.

The undeformed alloy shows a longer aging time to achieve the peak hardness for both aging temperatures. In contrast, the deformed alloy shows a considerable increase in the hardness values with an increase in the degree of deformation. At the same time, the aging time required to achieve the peak hardness is lowered. At 100°C, the aging time for deformed specimens with 4, 8 and 12% deformation reduced by 20, 27 and 34%, respectively, as compared to the undeformed specimen. Similarly, at 180°C, the aging time for deformed specimens reduced by 19, 30 and 38%, respectively.

The comparison between the hardness and aging time values of alloy subjected to both the IATs clearly shows higher hardness and aging time for the specimens (deformed or undeformed) aged at 100°C. However, at a higher aging temperature of 180°C, the specimens achieved peak hardness with reduced aging time. The higher peak hardness at lower IAT is caused by the occurrence of additional intermediate

Table 2. Peak hardness of AA6061 post thermomechanical treatment.

Deformation (%)	Aging temperature of 100°C		Aging temperature of 180°C	
	Peak hardness value (HV)	Aging time (h)	Peak hardness value (HV)	Aging time (h)
0	101.97	14.5	93.90	13.0
4	108.53	11.5	101.87	10.5
8	115.43	10.5	111.20	9.0
12	120.07	9.5	118.83	8.0

stages for spontaneous separation of solute atoms which is when precipitation of secondary phases occurs. In the case of specimens aged at higher IAT, the aging kinetics is accelerated. Therefore, the diffusion rate is higher with reduced intermediate stages where the precipitation of the secondary hard phase occurs²⁶. This results in lower peak aging duration at higher IATs.

The tensile test was carried out to find the (UTS) of AA6061 solutionized and heat-treated specimens. The hardness values and strength variation show similar behaviour concerning the same heat treatment conditions. The ultimate tensile strength of the as-cast and solutionized specimens were found to be 147.8 and 120.2 MPa, respectively. The study carried by Kumar and Murugan revealed the UTS value of AA6061 alloy to be in the range of 160–165 MPa³⁴. The UTS of 6061 Al alloy was in the range of 130–135 MPa as observed by Auradi et al.³⁵. As expected, the comparison of the UTS values of as-cast alloy shows a considerable difference which is because of the variation in the composition of the alloy and varied parameters of the casting process for the alloy. The solutionizing of the specimen results in a supersaturated solid solution that leads to increased softness which is direct proof of achieving lower tensile strength than the as-cast specimen²⁶. To enhance the strength of the material the secondary phase must be well distributed in the aluminium rich solid solution, which requires proper selection of aging parameters²⁸. Figure 5 shows the UTS of AA6061 specimens subjected to different deformations and IATs at peak-aged conditions.

From Figure 5, it may be observed that after the age hardening treatment at IATs of 100 and 180°C, the UTS increased by about 15 and 3%, respectively, compared to the UTS of the as-cast specimen. Similarly, compared to conventional age hardened specimens, the thermomechanically treated specimens show a maximum of 49% increase in UTS at both the IATs of 100 and 180°C. It may also be noted that the UTS reduces by 10–11% in the alloy with or without deformation by increasing the IAT from 100 to 180°C.

The fractured surface of the tensile specimens was examined under a scanning electron microscope (SEM) to understand the mode of failure and the microstructural effect on the properties. The tensile fracture surface of conventionally peak aged AA6061 without deformation (Figure 6) shows a typical ductile dominant failure mode at both 100 and 180°C. During age hardening, a large number of nucleation sites

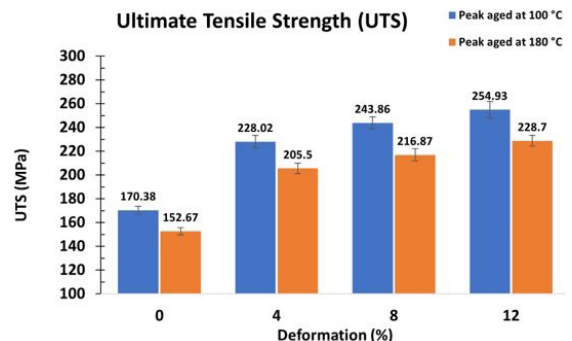


Figure 5. Variation of ultimate tensile strength with the increase in deformation at peak-aged conditions.

are generated, leading to the formation of a large number of micro voids. The amalgamation of these micro voids results in the formation of dimples³⁶. At lower aging temperatures, the dimples are of uniform size, and the intergranular crack propagating in different directions (Figure 6a) shows that the specimen is ductile. The impressions of the river pattern show that brittle failure mode is also in process. At lower aging temperatures, since the dimples are of the same size, the considerable plastic flow of metal is predominant before failure. At high temperature aging, a mix of coarse and fine dimples is formed along with a shallow river pattern (Figure 6b). This is the indication of easy failure of the specimen with dominant ductile mode while the tendency of brittle mode failure is meagre.

3.2. Mechanical characterization of the alloy subjected to nLTMT process

The study was further extended to find a new LTMT sequence to enhance the mechanical properties of the alloy further. Hence, the LTMT sequence was varied by carrying out the cold rolling in two steps, with each rolling followed by partial aging of specimens at IATs of 100 and 180°C. The details of the aging time at both the IATs in each step is shown in Table 3.

Figures 7a and 7b show the variation in the peak hardness of the alloy subjected to LTMT and the nLTMTs at both the IATs of 100 and 180°C, respectively. The peak hardness of the alloys processed through nLTMT1 when compared with

LTMT alloy indicates a maximum of 3 and 5% increase in peak hardness at 100 and 180°C, respectively. Likewise, the nLTMT2 and nLTMT3 alloys reveal a gradual increase in the peak hardness, with the latter showing better results amongst all the heat treatment processes. The peak hardness of the nLTMT3 processed alloy increased by a maximum of 7% considering both the aging temperatures.

Figures 8a and 8b show the variation in the tensile strength of the alloy processed through LTMT and different nLTMT processes. Similar to the peak hardness values, the tensile strength of the alloy subjected to nLTMT3 showed the best results with the maximum increase in strength of 9 and 13% as compared to alloy subjected to LTMT process at 100 and 180°C IATs, respectively. In the nLTMT treatments the first stage of the cold rolling of the alloy increases the dislocation density in the structure of the material. When the cold worked material is subjected to aging treatment the strengthening mechanism occurs due to the increased nucleation sites available for the formation of precipitates. Additionally, the second stage of the cold working and aging treatment enhances the strength of the alloy. Thus, the gradual increase in the strength of the alloys processed through various nLTMT processes in comparison to alloy subjected to LTMT process is evident at both the IATs.

The nLTMT processed alloy revealed excellent hardness and strength for lower temperature (100°C) aging compared to aging at higher temperatures (180°C). The nLTMT processed alloy aged at 100°C indicated 6-8% increase in UTS and

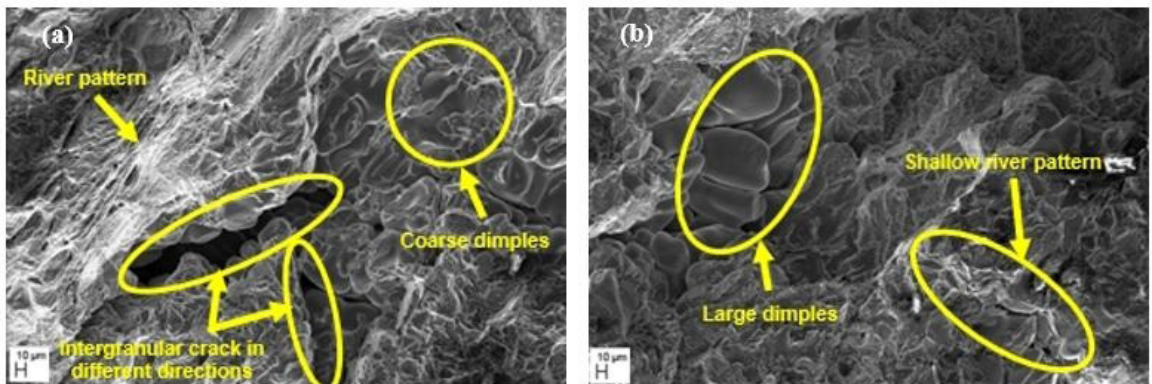


Figure 6. SEM fractographs of precipitation hardened AA6061 peak aged at (a) 100°C and (b) 180°C.

Table 3. Various aging time at both IATs for the nLTMT process.

Process type	Amount of Deformation $C_1 = C_2$ (%)	$D_1:D_2$	Aging Time at 100°C (h)			Aging Time at 180°C (h)		
			D_1	D_2	LTMT (D_1+D_2)	D_1	D_2	LTMT (D_1+D_2)
nLTMT1	2	1:1	5.75	5.75	11.5	5.25	5.25	10.5
	4		5.25	5.25	10.5	4.50	4.50	9.0
	6		4.75	4.75	9.5	4.00	4.00	8.0
nLTMT2	2	1:2	3.83	7.67	11.5	3.50	7.00	10.5
	4		3.5	7	10.5	3.00	6.00	9.0
	6		3.17	6.33	9.5	2.67	5.33	8.0
nLTMT3	2	2:1	7.67	3.83	11.5	7.00	3.50	10.5
	4		7	3.5	10.5	6.00	3.00	9.0
	6		6.33	3.17	9.5	5.33	2.67	8.0

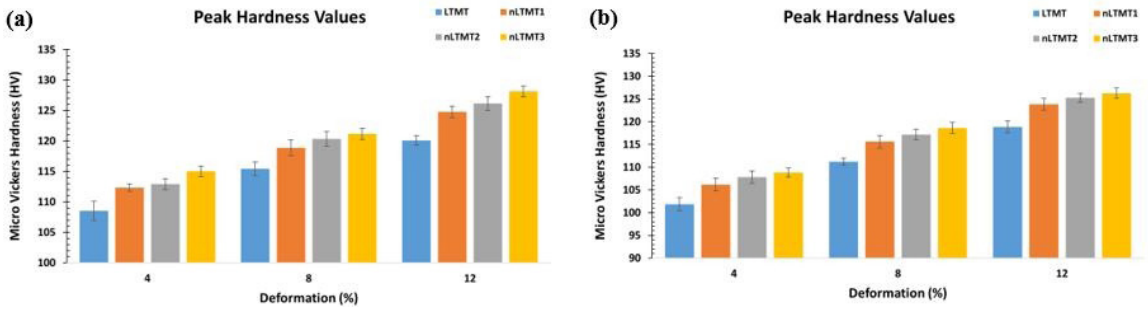


Figure 7. Variation of peak hardness with the increase in deformation at (a) 100°C and (b) 180°C.

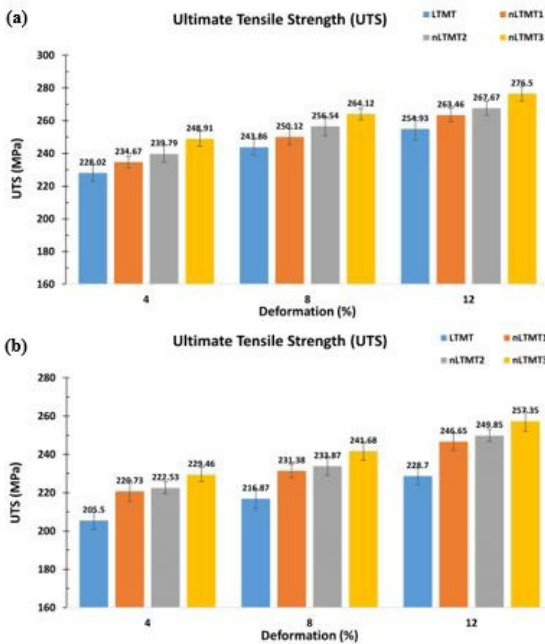


Figure 8. Variation of ultimate tensile strength with the increase in deformation at (a) 100°C and (b) 180°C.

2-3% increase in hardness when compared to the alloy aged at 180°C. In the case of alloy subjected to nLTMT3 with 4% deformation (Figure 9), the dimples observed were dent/cup-shaped and randomly oriented. Some dimples were also found to be elongated. The elongated cup-like dimples with different orientations are the indication of strain hardening feature in the metal. Several small river patterns (Figure 9a) indicate higher strength due to the deformation effect. A very small, unevenly oriented large density river pattern is observed (Figure 9b) at a higher aging temperature, indicating ductile dominant failure mode³⁷.

As the degree of deformation increases, at lower aging temperature, the severe strain hardened feature is observed (Figure 10a) due to the orientation of cup-like dimples and river pattern in a particular direction. The river pattern cluster also includes the facets. The presence of the facet is an indication of brittle failure. Figure 10b reveals the brittle dominance in failure without any dimples. Some clusters of river patterns are also observed, indicating a mixed-mode of failure. Mixed-mode of fracture is predominant in all the peak aged LTMTs, although in certain locations brittle

fracture exists. The number of sites with voids and dimples is enhanced as the deformation degree increases. At some locations, elongated dimples are noticed, ascribed to shear or tear fracture in a localized region. It is also noted that some of the dimples are shallow and can be caused by the amalgamation of micro voids. Coalescence of micro voids due to shear results in shallow dimples, as noticed in a few regions in the fractographs. The size and density of dimples are influenced by the dissemination of nucleation sites/defects. Dimples of different sizes are generated due to non-uniformity in the size of these defects or nucleation sites³⁷. They tend to be elongated in a few areas on the fracture surface, relying on loading conditions.

At 12% deformation specimen (Figure 11) displays many river patterns with facets. Figure 11a is filled with river patterns with fewer uneven facets. The river pattern indicates excellent strength and hardness, with the facets indicating brittle failure. In Figure 11b, the larger facets are observed along with lesser river pattern density than its counterpart (Figure 11a). This is an indication of brittle dominant failure. In its entirety, it is observed that the failure mode in the alloy is ductile-brittle (combined) in nature. As the degree of deformation increases or the aging temperature decreases, the brittle failure mode dominates in the combined domain.

3.3. Effect of deformation sequence on the hardness and tensile strength of AA6061

To explore the possibility of an alternate deformation sequence in the heat treatment cycle, the best outcome, i.e. 12% total degree of deformation and 100°C aging temperature (for the expected maximum hardness and UTS), are considered. To understand the influence of the degree of deformation on the peak hardness of the alloy by alternate deformation sequence, two curves of the LTMT process with 0 and 4% deformation at 100°C IAT was selected. In these two curves, two clear, distinct peaks are visible from Figure 4a, and the hardness values are shown in Table 4. In both the curves during aging after the first peak, there is a temporary relaxation in the strengthening tendency, i.e. reduction in hardness for a short duration. This phenomenon is due to the rearrangement of atoms in the unit cell when metastable phase reformation occurs and when the precipitates coalesce and lose coherence^{26,28}.

In the first case (0% deformation) the alloy specimen was subjected to LTMT at lower aging temperature (100°C) with intermediate three-step deformation at the aging time of

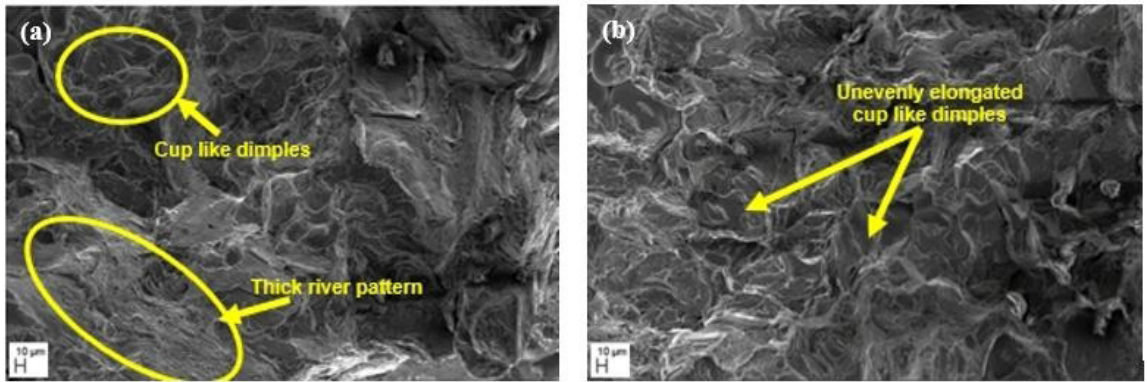


Figure 9. SEM fractographs of nLTMT3 processed AA6061 with 4% deformation peak aged at (a) 100°C and (b) 180°C.

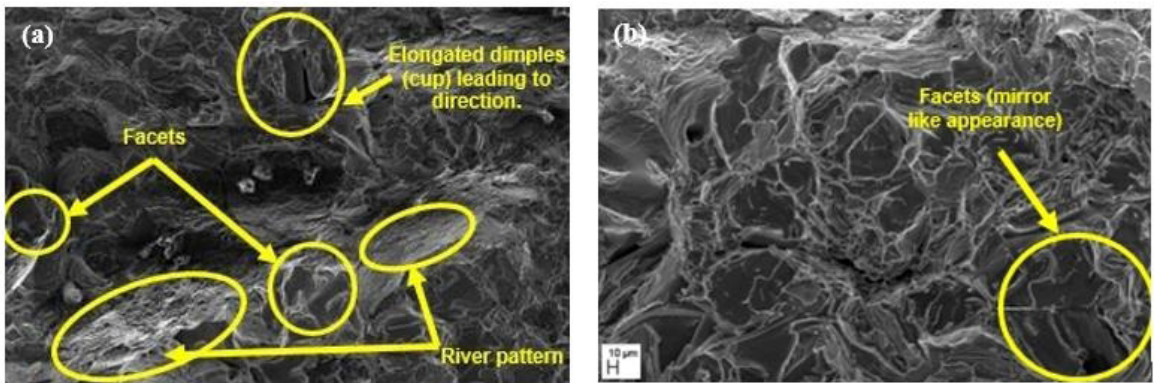


Figure 10. SEM fractographs of nLTMT3 processed AA6061 with 8% deformation peak aged at (a) 100°C and (b) 180°C.

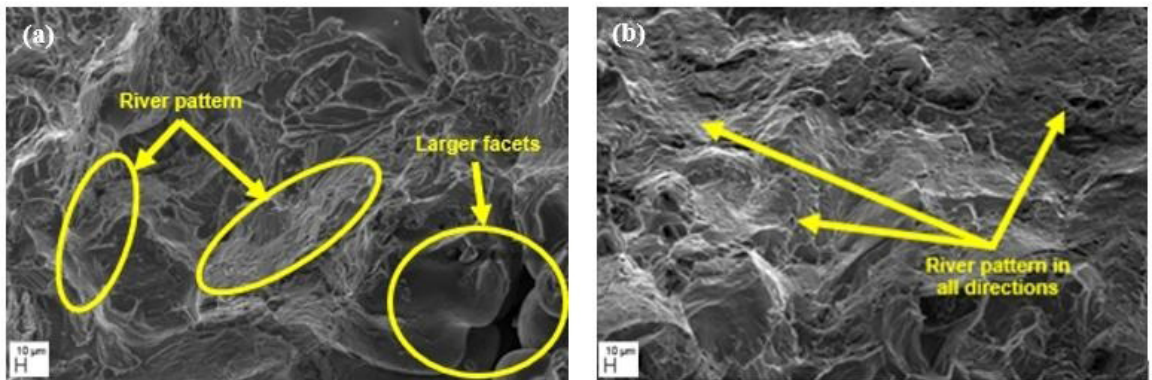


Figure 11. SEM fractographs of nLTMT3 processed AA6061 with 12% deformation peak aged at (a) 100°C and (b) 180°C.

Table 4. Hardness values and time of 0 and 4% deformed LTMT specimens at 100°C.

		1 st peak	Peak Hardness
LTMT specimen with 0% deformation	Hardness Values (HV)	97.60	101.97
	Time (h)	9.5	14.5
LTMT specimen with 4% deformation	Hardness Values (HV)	105.70	108.53
	Time (h)	9	11.5

9.5, 12 and 14.5 h with each deformation of 4% (Figure 12). The hardness value measured at 14.5 h post third deformation (with total deformation of 12%) is 125.74 HV, a 23% increase compared to 101.97 HV of the alloy aged without any deformation (Table 4). Similarly, the UTS of the alloy was found to be 239.56 MPa which is a 40% increase from 170.38 MPa of the alloy without deformation. Thus, with an increase in degree of deformation, the hardness and tensile strength of the alloy increases with the same aging duration.

Likewise, at the aging of the 1st peak, the 0% deformation alloy is subjected to 12% deformation at the 1st peak aging

condition after solutionising and aged for 14.5 h at 100°C (Figure 13). The peak hardness recorded is 121 HV, and peak UTS is 212.5 MPa, which is less than the previous treatment cycle.

The same is further substantiated by repeating the process wherein the specimen is cold rolled at 4% post solution treatment and quenching. The specimen is aged at 100°C

for 9 h, which is the time taken for achieving the 1st peak for 4% LTMT specimen. The second and third deformation during the aging is carried at the aging time of 10.25 and 11.5 h, respectively, with each deformation of 4% (Figure 14). The hardness value measured at 11.5 h is 130.34 HV which is 21% higher than the previous value of 108.53 HV with only 4% deformation. Similarly, the UTS showed an increase

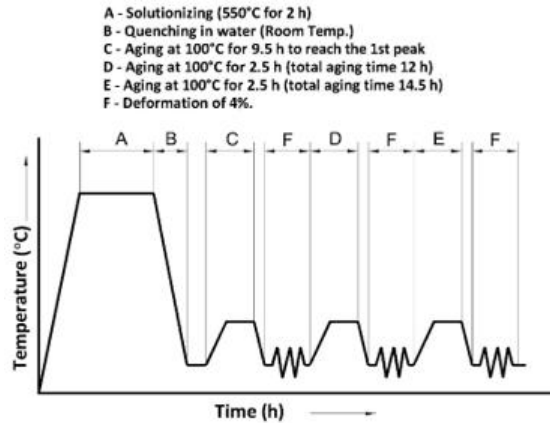


Figure 12. Modified LTMT cycle for 0% deformed AA6061 at 100°C IAT.

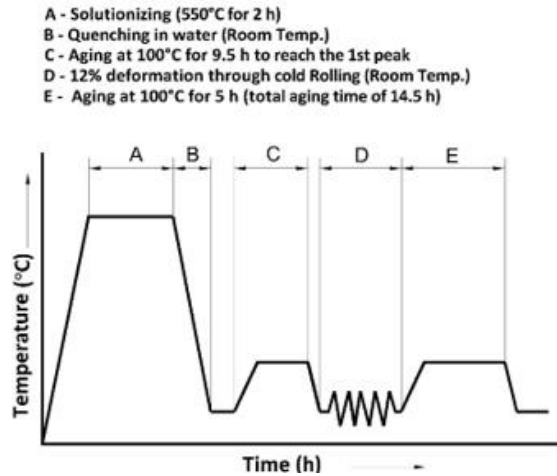


Figure 13. Modified LTMT cycle for AA6061 at 100°C IAT with preliminary aging.

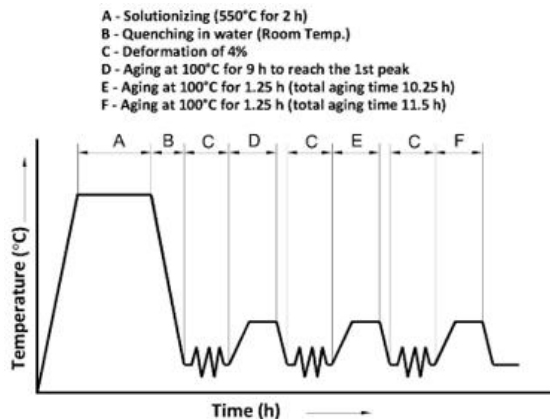


Figure 14. Modified LTMT cycle for 4% deformed AA6061 at 100°C IAT.

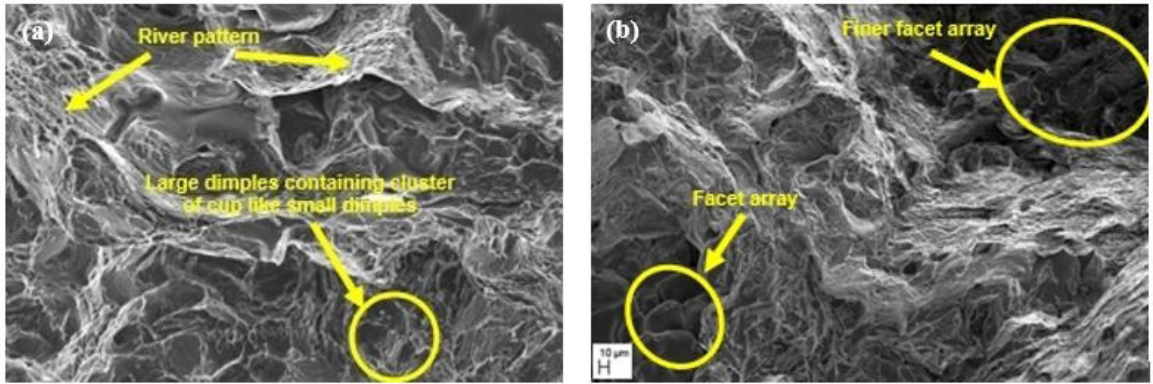


Figure 15. SEM fractographs of LTMT processed AA6061 with 12% deformation peak aged at 100°C (a) with and (b) without preliminary deformation.

Table 5. Hardness and UTS of Modified LTMT specimens at 100°C.

Heat treatment sequence	Peak hardness (HV)	UTS (MPa)
Figure 12	125.74	239.56
Figure 13	121	212.5
Figure 14	130.34	265.4

of 37% from 228.02 to 265.4 MPa. The hardness and UTS obtained by these alternate sequences are shown in Table 5. These deformation sequences show that the pre-deformation (4%) concentrated approach gives a better result, which means the interaction of strain hardening with the nucleation sites generated by pre-deformation played a more significant role in the increase in hardness and UTS.

The fracture surface of the specimens subjected to the LTMT sequence in Figure 14 is shown in Figure 15. Figure 15a shows river patterns, facets, and large-sized clusters of cup-like dimples. A large variety of such dimples are observed, which is an indication of excellent strength and hardness. With the same deformation of 12% but without preliminary deformation, Figure 15b shows a finer facet array. A large river pattern is the indication of strain hardening. The fracture analysis shows excellent mechanical properties of the alloy with preliminary deformation, aging and LTMT at the first peak over prior aging and LTMT at the first peak. Thus, pre-deformation is essential for attaining excellent strength and hardness response.

4. Conclusion

Following the studies on the hardness and tensile strength and fracture surface analysis of the AA6061 processed through precipitation hardening, and various low temperature thermomechanical treatment, the subsequent conclusions were arrived at:

- AA6061 was successfully subjected to LTMT and alternate LTMT sequences yielding better results than the conventional heat treatment process. The hardness and strength of the alloy increased with the increase in degree of deformation.
- The hardness and tensile tests conducted on the alloy revealed better properties at the lower aging

temperature of 100°C. This was true in all the cases wherein the alloy was processed through conventional aging, LTMT and nLTMT sequences.

- Hardness and UTS of the alloy subjected to nLTMT improved by 25% and 60%, respectively, compared to alloy subjected to conventional aging treatment. Fracture surface analysis of nLTMT processed alloy showed a mixed-mode of failure (brittle and ductile) with brittle mode dominating with the increase in degree of deformation of the alloy.
- The modified LTMT sequence showed the significant effect of pre-deformation on the alloy's hardness and UTS, which is verified by the fracture surface analysis. The hardness and strength of the alloy subjected to modified LTMT sequence with 4% deformation showed an increase of 21 and 37% respectively over LTMT processed alloy.

5. References

1. Esmaeili S, Lloyd DJ, Jin H. A thermomechanical process for grain refinement in precipitation hardening AA6xxx aluminum alloys. *Mater Lett.* 2011;65(6):1028-30.
2. Fare S, Lecis N, Vedani M. Aging behaviour of Al-Mg-Si alloys subjected to severe plastic deformation by ECAP and cold asymmetric rolling. *J Metall.* 2011;2011:959643.
3. Smolej A, Gnamus M, Slacek E. The influence of the thermomechanical processing and forming parameters on superplastic behaviour of the 7475 aluminium alloy. *J Mater Process Technol.* 2001;118(1):397-402.
4. Huang YJ, Chen ZG, Zheng ZQ. A conventional thermo-mechanical process of Al-Cu-Mg alloy for increasing ductility while maintaining high strength. *Scr Mater.* 2011;64(5):382-5.
5. Mishra VD, Rao BC, Murthy H. Enhancement of mechanical properties by cold-rolling of Al6061. *Mater Today Proc.* 2018;5(2):8263-70.
6. Yu HL, Tieu AK, Lu C, Liu XH, Godbole A, Kong C. Mechanical properties of Al-Mg-Si alloy sheets produced using asymmetric cryorolling and ageing treatment. *Mater Sci Eng A.* 2013;568:212-8.
7. Kim WJ, Wang JY. Microstructure of the post-ECAP aging processed 6061 Al alloys. *Mater Sci Eng A.* 2007;464(1-2):23-7.
8. Huang Y, Yan X, Qiu T. Microstructure and mechanical properties of cryo-rolled AA6061 Al alloy. *Trans Nonferrous Met Soc China.* 2016;26(1):12-8.

9. Kim JK, Jeong HG, Hong SI, Kim YS, Kim WJ. Effect of aging treatment on heavily deformed microstructure of a 6061 aluminum alloy after equal channel angular pressing. *Scr Mater*. 2001;45(8):901-7.
10. Khan AS, Meredith CS. Thermo-mechanical response of Al 6061 with and without equal channel angular pressing (ECAP). *Int J Plast*. 2010;26(2):189-203.
11. Rominiyi AL, Oluwasegun KM, Olawale JO, Shongwe MB, Adetunji AR. Effect of post-ECAP aging on the microstructure, hardness and impact behaviour of 6061 Al alloy. *Mater Today Proc*. 2021;38:1031-4.
12. Lee SH, Saito Y, Sakai T, Utsunomiya H. Microstructures and mechanical properties of 6061 aluminum alloy processed by accumulative roll-bonding. *Mater Sci Eng A*. 2002;325(1-2):228-35.
13. Yu H, Su L, Lu C, Tieu K, Li H, Li J, et al. Enhanced mechanical properties of ARB-processed aluminum alloy 6061 sheets by subsequent asymmetric cryorolling and ageing. *Mater Sci Eng A*. 2016;674:256-61.
14. Rezaei MR, Toroghinejad MR, Ashrafizadeh F. Effects of ARB and ageing processes on mechanical properties and microstructure of 6061 aluminum alloy. *J Mater Process Technol*. 2011;211(6):1184-90.
15. Xu C, Horita Z, Langdon TG. The evolution of homogeneity in an aluminum alloy processed using high-pressure torsion. *Acta Mater*. 2008;56(18):5168-76.
16. Mohamed IF, Lee S, Edalati K, Horita Z, Hirotsawa S, Matsuda K, et al. Aging behavior of Al 6061 alloy processed by high-pressure torsion and subsequent aging. *Metall Mater Trans, A Phys Metall Mater Sci*. 2015;46(6):2664-73.
17. Takeda M, Ohkubo F, Shirai T, Takeda M. Stability of metastable phases and microstructures in the ageing process of Al-Mg-Si ternary alloys. *J Mater Sci*. 1998;33(9):2385-90.
18. Edwards GA, Stiller K, Dunlop GL, Couper MJ. The precipitation sequence in Al-Mg-Si alloys. *Acta Mater*. 1998;46(11):3893-904.
19. Murayama M, Hono K. Pre-precipitate clusters and precipitation processes in Al-Mg-Si alloys. *Acta Mater*. 1999;47(5):1537-48.
20. Matsuda K, Sakaguchi Y, Miyata Y, Uetani Y, Sato T, Kamio A, et al. Precipitation sequence of various kinds of metastable phases in Al-1.0 mass% Mg, Si-0.4 mass% Si alloy. *J Mater Sci*. 2000;35(1):179-89.
21. Gupta AK, Lloyd DJ, Court SA. Precipitation hardening in Al-Mg-Si alloys with and without excess Si. *Mater Sci Eng A*. 2001;316(1-2):11-7.
22. Niranjani VL, Kumar KH, Sarma VS. Development of high strength Al-Mg-Si AA6061 alloy through cold rolling and ageing. *Mater Sci Eng A*. 2009;515(1-2):169-74.
23. Sanyal S, Chabri S, Chatterjee S, Bhowmik N, Metya AK, Sinha A. Tribological behavior of thermomechanically treated Al-Mg-Si alloy by nanoscratch measurements. *Tribol Int*. 2016;102:125-32.
24. Demir H, Gunduz S. The effects of aging on machinability of 6061 aluminium alloy. *Mater Des*. 2009;30(5):1480-3.
25. Ozturk F, Sisman A, Toros S, Kilic S, Picu RC. Influence of aging treatment on mechanical properties of 6061 aluminum alloy. *Mater Des*. 2010;31(2):972-5.
26. Avner SH. Introduction to physical metallurgy. 2nd ed. New York: McGraw-Hill; 2012.
27. Pogatscher S, Antrekowitsch H, Ebner T, Uggowitzer PJ. The role of co-clusters in the artificial aging of AA6061 and AA6060. In: Suarez CE, editor. Light metals. Cham: Springer; 2012. p. 415-20.
28. Rajan TV, Sharma CP, Sharma A. Heat treatment: principles and techniques. 2nd ed. New Delhi: PHI Learning Pvt. Ltd.; 2012.
29. Mirzakhani B, Mansourinejad M. Tensile properties of AA6061 in different designated precipitation hardening and cold working. *Procedia Eng*. 2011;10:136-40.
30. Mansourinejad M, Mirzakhani B. Influence of sequence of cold working and aging treatment on mechanical behaviour of 6061 aluminum alloy. *Trans Nonferrous Met Soc China*. 2012;22(9):2072-9.
31. Gopi B, Krishna NN, Venkateswarlu K, Sivaprasad K. Influence of rolling temperature on microstructure and mechanical properties of cryorolled Al-Mg-Si alloy. *World Acad Sci Eng Technol*. 2012;61:731-5.
32. Kolar M, Pedersen KO, Gulbrandsen-Dahl S, Teichmann K, Marthinsen K. Effect of pre-deformation on mechanical response of an artificially aged Al-Mg-Si alloy. *Mater Trans*. 2011;52(7):1356-62.
33. Yousefi A, Eivani AR, Boutorabi SMA, Jafarian HR. Effect of pre-deformation cooling rate on the age-hardening response of ultrafine grained AA6063. *Mater Sci Eng A*. 2018;713:180-9.
34. Kumar BA, Murugan N. Metallurgical and mechanical characterization of stir cast AA6061-T6-AlNp composite. *Mater Des*. 2012;40:52-8.
35. Auradi V, Rajesh GL, Kori SA. Preparation and evaluation of mechanical properties of 6061Al-B4Cp composites produced via two-stage melt stirring. *Mater Manuf Process*. 2014;29(2):194-200.
36. Sharma S, Gowrishankar MC, Hiremath P, Shettar M, Gurumurthy BM. Tensile fractography of artificially aged Al6061-SiC+B₄C hybrid composites. *Mater Sci Forum*. 2020;995:3-8.
37. Shankar MCG, Sharma SS, Kini UA, Hiremath P, Gurumurthy. Microstructure and fracture behaviour of two stage stir cast Al6061-SiC composites. *J Mater Environ Sci*. 2017;8(1):257-63.